1330 *Chem. Mater.* **1994,** *6,* 1330–1336

Structure and Solid-State Reactivity of 2-Aminopyridinium Propynoate

Kraig A. Wheeler[†] and Bruce M. Foxman[*,‡]

Department of Chemistry, Delaware State University, Dover, Delaware 19901, and Department of Chemistry, Brandeis University, Waltham, Massachusetts 02254-9110

Received February 2, 1994[⊗]

The cocrystalline salt 2-aminopyridinium propynoate (4) was prepared by mixing 2-aminopyridine and propynoic acid in acetone. Heating solid 4 at 100 °C for 2 h leads to a 9:10 mixture of 2-imino-1-2*H*-pyridine-(*E*)-acrylic acid (5) and 2*H*-pyrido[1,2-*a*]pyrimid-2-one (6). The reaction is one of two rare examples of such an addition reaction in the solid state and is highly chemospecific compared to the analogous reaction in solution. Structure–reactivity relationships for 4 as well as the crystal structure of 5 are discussed. Crystal data: 4: monoclinic, space group $P2_1/n$, $a = 11.503(3)$, $b = 7.004(2)$, $c = 11.052(3)$ Å; $\beta = 110.19(3)°$; $R = 0.047$, $R_w = 0.047$ for 799 data for which $I > 1.96\sigma(I)$. 5: monoclinic, space group $P2_1/c$, $a = 15.458(4)$, $b = 15.506(4)$, $c = 7.133(2)$ Å; $\beta = 102.00(3)°$; $R = 0.040$, $R_w = 0.044$ for 1566 data for which $I > 1.96\sigma(I)$.

Introduction

In 1990 we read one of Professor Peggy Etter's many interesting papers,[1] viz., "The Use of Cocrystallization as a Method of Studying Hydrogen Bond Preferences of 2-Aminopyrimidine". In addition to providing a window to understanding the parameters that influence hydrogen-bond formation and patterns, there was an additional message for us, not realized until quite recently. For the 1:1 crystal of 2-aminopyrimidine with succinic acid, a relatively short unit-cell translation, 5.045 Å, was observed. Only later did we realize that, with careful study, it should be possible to produce unusual phases containing cocrystals of planar amine/pyridine molecules together with reactive unsaturated carboxylic acids. Further, we surmised, these unusual phases might contain reactive molecules in close proximity; then, solid-state reactivity would be observed. As we scientists reflect on Professor Etter's published work, it is clear that we will again and again find many gems which will continue to inspire us; this is only part of her greatness.

Initially, we hoped to use the new phases to explore the solid-state polymerization of pyridinium salts of propynoic acid. Metal salts of propynoic acid are very sensitive to ^{60}Co γ-rays,[2-4] while there was not much information on the solid-state reactivity of organic monoacetylenes.[5] The idea inspired by Etter and Adsmond's paper was successful: a phase containing acetylene moieties in close proximity was readily prepared, for example, by mixing propynoic acid and 4-(1-pyrrolidino)pyridine in ethanol. However, this phase was insensitive to ^{60}Co γ-rays, despite the fact that short acetylene–acetylene contacts were observed between the propynoate anions. Although the material was not radiation-sensitive, it nonetheless exhibited a new type of solid-state reactivity.[6] Heating the resultant cocrystalline solid 1 converted it, in high yield,

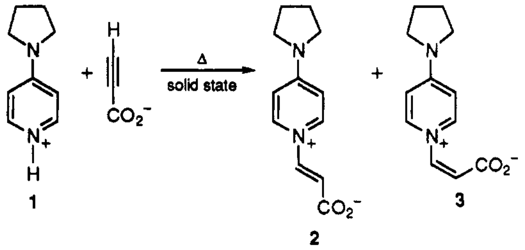

to a 19:1 mixture of (*E* and *Z*)-4-(1-pyrrolidino)-pyridinium-1-acrylate (**2, 3**). To the best of our knowledge, this represented the first example of the addition of a pyridine moiety to an acetylene in the solid state. During our investigation of the solid-state reaction, we discovered that the room-temperature structure transformed to a high-temperature phase before reaction occurred; it has not yet been possible to obtain crystals of the high-temperature material.[6] Thus, structure–reactivity relationships for this solid-state addition reaction remain unknown.

The present work reports the structure, solid-state reactivity and product analysis for the cocrystalline salt 2-aminopyridinium propynoate (4). While the unit cell for 4 has no short translations, an analysis of the packing shows that short acetylene–acetylene contacts are a major feature of the crystal structure. Again, the all-organic material is not sensitive to ^{60}Co γ-rays. However, when 4 is heated in the solid state, addition products 5 and 6 are formed; no phase transformation occurs prior to reaction. Thus, the X-ray structure determination of compounds 4 and 5 provide an opportunity to examine

---

[†] Delaware State University.

[‡] Brandeis University.

[⊗] Abstract published in *Advance ACS Abstracts,* August 15, 1994.

(1) Etter, M. C.; Adsmond, D. A. *J. Chem. Soc., Chem. Commun.* **1990,** 589.

(2) Booth, C. A.; Jaufmann, J. D.; Foxman, B. M. *Polym. Prepr. (Am. Chem. Soc., Div. Polym. Chem.)* **1986,** *54,* 206.

(3) Booth, C. A.; Foxman, B. M.; Jaufmann, J. D. In *Crystallographically Ordered Polymers*; Sandman, D. J., Ed.; ACS Symposium Series 337; American Chemical Society: Washington, DC, 1987; pp 95–105.

(4) Brodkin, J. S.; Foxman, B. M. *J. Chem. Soc., Chem. Commun.* **1991,** 1073.

(5) Sandman, D. J.; Hamill, G. P.; Samuelson, L. A.; Foxman, B. M. *Mol. Cryst. Liq. Cryst.* **1984,** *106,* 199. Sandman, D. J.; Velazquez, C. S.; Hamill, G. P.; Preses, J. M.; Weston, Jr., R. E.; Foxman, B. M. *Mol. Cryst. Liq. Cryst.* **1988,** *156,* 103.

(6) Wheeler, K. A.; Foxman, B. M. *Mol. Cryst. Liq. Cryst.* **1992,** *211,* 347.

0897-4756/94/2806-1330$04.50/0

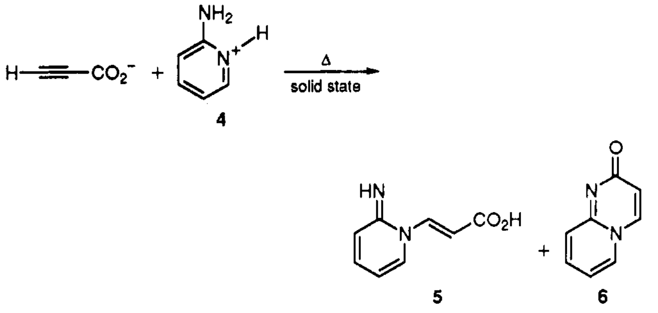

structure–reactivity relationships for an unusual solid-state addition reaction.

Experimental Section

Instrumentation. Melting points were determined on a Laboratory Devices Mel-Temp apparatus and are uncorrected. IR spectra were recorded using Mattson Cygnus 100 FT-IR and Perkin-Elmer 683 spectrophotometers. ^{1}H and ^{13}C NMR spectra were recorded on Varian EM-390 (90 MHz) and XL-300 (300 MHz) spectrometers. Chemical shifts are given in parts per million downfield from 3-(trimethylsilyl)-1-propanesulfonic acid sodium salt. The following abbreviations are used to indicate signal multiplicity (NMR) or spectral characteristics (IR): s, singlet; d, doublet; t, triplet; q, quartet; m, multiplet; b, broad; sh, shoulder. A Gammacell 220 Irradiator (Atomic Energy of Canada, Ltd.) equipped with a ^{60}Co source was used for all γ-irradiation experiments. The nominal activity of the source at the time of the experiments was 0.0403 Mrad/h.

2-Aminopyridinium Propynoate (4). To a stirred solution of 2-aminopyridine (3.00 g, 3.19 mmol) and acetone (20 mL) at 25 °C was added dropwise (5 min) a solution of propynoic acid (2.34 g, 3.35 mmol) in acetone (5 mL). As the mixture was stirred (30 min), a colorless flocculent solid appeared. The precipitate was isolated by vacuum filtration (20 Torr) and dried in vacuo (0.25 Torr) over $CaSO_4$ to afford 4.46 g (87%) of 4 as colorless crystals: mp 121–123 °C; IR (KBr) 3205, 3090, 2995, 2086, 1635 cm^{-1}; ^{1}H NMR (D_2O) δ 7.92 (1 H, ddd, J = 10.0, 7.5, 1.5 Hz), 7.80 (1 H, dd, J = 7.5, 1.5 Hz), 7.01 (1 H, dd, J = 10.0, 1.0), 6.86 (1 H, ddd, J = 7.5, 7.5, 1.0), 3.08 (1 H, s).

2-Imino-1-2*H*-pyridine-(*E*)-acrylic Acid and 2-*H*-Pyrido-[1,2-*a*]pyrimid-2-one (5 and 6). At 760 Torr, 153 mg (0.93 mmol) of crystalline 4 was heated at 80 °C for 6 h to afford a brown opaque solid (150 mg). ^{1}H NMR analysis of the solid showed a 1:1.4 ratio of 5 and 6 in 80% combined yield.

5: mp 220–221 °C; IR (KBr) 3460, 3080, 1695, 1640, 1560, 960 cm^{-1}; ^{1}H NMR (1:1 D_2O:DMSO-d_6) δ 8.0–7.8 (2 H, m), 7.54 (1 H, d, J = 13.7 Hz), 7.11 (1 H, d, J = 9.5 Hz), 6.97 (1 H, dd, J = 7.1, 7.1 Hz), 6.57 (1 H, d, J = 13.7 Hz); ^{13}C NMR (D_2O) δ 173.8 (C), 156.4 (C), 146.3 (CH), 144.2 (CH), 137.4 (CH), 137.2 (CH), 118.7 (CH), 116.4 (CH).

6: IR (KBr) 3080, 1673, 1645, 705 cm^{-1}; ^{1}H NMR (1:1 D_2O:DMSO-d_6) δ 8.51 (1 H, d J = 7.7 Hz), 8.32 (1 H, dd, J = 6.6, 1.5 Hz), 7.88 (1 H, ddd, 8.7, 6.6, 1.5 Hz), 7.38 (1 H, dd, J = 8.7, 1.0 Hz), 7.20 (1 H, ddd, J = 6.6, 6.6, 1.0 Hz) 6.68 (1 H, d, J = 7.7 Hz); ^{13}C NMR (D_2O) δ 173.4 (C), 154.6 (C), 141.9 (CH), 139.6 (CH), 132.3 (CH), 125.2 (CH), 117.9 (CH), 117.5 (CH).

X-ray Structure Determinations. Colorless platelike crystals of 4 were grown by slow evaporation of an acetone solution. Weissenberg and oscillation photographs as well as polarized light microscopy indicated the crystal to be of good quality. To correspond to the cell chosen from Weissenberg photography, data were collected in space group $B2_1/c$, and the structure was solved in this space group. The final refinement was carried out after the structure had been transformed to the cell of one-half the original volume, in space group $P2_1/n$. Crystals of 5 were grown by slow evaporation of an aqueous solution. Data were collected in space group $P2_1/a$, and the structure was solved in this space group. The final refinement was carried out after the structure had been transformed to space group $P2_1/c$. The final choices of $P2_1/n$ and $P2_1/c$ for 4 and 5, respectively, correspond to the monoclinic unit cells with the angle β nearest to 90°. Operations on the Syntex $P2_1$ diffractometer were performed as described previously.[7,8] The analytical scattering factors of Cromer and Waber were used; real and imaginary components of anomalous scattering were included in the calculations.[9] Complete experimental detail is presented in Table 1, atomic coordinates in Tables 2 (4) and 3 (5), and selected bond lengths for both structures in Table 4. Tables of anisotropic displacement parameters, complete molecular geometry for both structures, calculated H atom coordinates, and observed and calculated structure amplitudes have been deposited as supplementary material (see paragraph at end of paper).

Results and Discussion

Crystal and Molecular Structure of 4. The salt formed from 2-aminopyridine and propynoic acid crystallizes as an eight-membered ring hydrogen-bonded heterodimer (Figure 1; N1–O1, 2.733(3) Å; N–H···O, 167(2)°; N2–O2, 2.835(3) Å; N–H···O, 177(2)°). The two subunits are not coplanar as previously reported for 2-aminopyridinium salicylate (3.9°)[10] but rather are skewed at an angle of 30.2(1)°. This value is considerably larger than that observed in the related stable phase, 2-aminopyridinium butynoate (15.2°);[11] this may reflect the influence of the C–H···O hydrogen bonds found in the structure of 4 (vide infra). The bond distances and angles of the propynoate subunit are similar to other fully dissociated propynoates.[2–4] The aminopyridinium cation appears to be in the iminium resonance form (7). The sum of the angles (360(2)°) around the amine nitrogen atom (N2) establishes the predominantly sp^2 character of that atom. The amino nitrogen-to-ring bond length, N2–C4 (1.325(4) Å), is significantly shorter than the N–C distances within the ring (1.349(3) and 1.358(4) Å). The C–C distances within the ring also show a deviation from those found in normal aromatic pyridine structures.[12] The distances C4–C5 (1.401(4) Å) and C6–C7 (1.395(4) Å) are considerably longer than those of C5–C6 (1.344(5) Å) and C7–C8 (1.336(4) Å). This evidence suggests a considerable degree of double-bond character between N2 and C4, which arises from the conjugation with the ring (resonance form 7). These features are very similar to those found for the cations in the 2-aminopyridinium salicylate[10] and butynoate[11] structures.

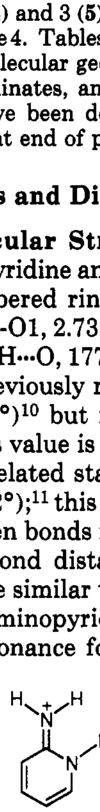

7

---

[7] Foxman, B. M. *Inorg. Chem.* **1978**, *17*, 1932. Foxman, B. M.; Mazurek, H. *Inorg. Chem.* **1979**, *18*, 113.

[8] *MolEN, An Interactive Structure Solution Procedure*; Enraf-Nonius: Delft, The Netherlands, 1990. Johnson, C. K. *ORTEP-II: A Fortran Thermal Ellipsoid Plot Program for Crystal Structure Illustrations, ORNL-5138*, 1976. Sparks, R. A.; et al. *Operations Manual, Syntex XTL Structure Determination Systems*; Syntex Analytical Instruments, Cupertino, CA, 1976. Sheldrick, G. M. *Acta Crystallogr., Sect. A: Found. Crystallogr.* **1990**, *46*, 467.

[9] Cromer, D. T.; Waber, J. T. In *International Tables for X-ray Crystallography*; Ibers, J. A., Hamilton, W. C., Eds.; Kynoch Press: Birmingham, England, 1974; Vol. IV, pp 99–101. Cromer, D. T.; Ibers, J. A. *Ibid.*; pp 148–150.

[10] Gellert, R. W.; Hsu, I.-N. *Acta Crystallogr., Sec. C: Cryst. Struct. Commun.* **1988**, *44*, 311.

[11] Wheeler, K. A.; Foxman, B. M. *Mol. Cryst. Liq. Cryst.* **1994**, *240*, 89.

[12] (a) Mootz, D.; Wussow, H. G. *J. Chem. Phys.* **1981**, *75*, 1520. (b) Longo, J.; Franklin, K. J.; Richardson, M. F. *Acta Crystallogr., Sect. B: Struct. Sci.* **1982**, *38*, 2721. (c) Weakley, T. J. R. *Inorg. Chim. Acta* **1982**, *63*, 161; (d) Ashida, T.; Hirokawa, S. *Acta Crystallogr.* **1965**, *18*, 122.

Table 1. X-ray Diffraction Data

	(A) Crystal Data at 21(1) °C	
compound	$(C_5H_7N_2)^+(C_3HO_2)^-$ (4)	$C_8H_8N_2O_2{\cdot}H_2O$ (5)
crystal system	monoclinic	monoclinic
space group	$P2_1/n[C^5_{2h}$; No. 14]	$P2_1/c[C^5_{2h}$; No. 14]
a, Å	11.503(3)	15.458(4)
b, Å	7.004(2)	15.506(4)
c, Å	11.052(3)	7.133(2)
β, deg	110.19(3)	102.00(3)
V, Å^3	835.7(8)	1672.4(15)
Z	4	8
crystal size, mm	0.13 × 0.21 × 0.55	0.13 × 0.42 × 0.63
formula wt	164.17	182.18
ρ_{calc}, g cm^{-3}	1.305	1.447
ρ_{obs}, g cm^{-3}	1.28(2)[a]	1.44(2)[a]
μ, cm^{-1} (Mo K$\bar{\alpha}$)	0.900	1.051
cell constant determination	seven pairs of ±(hkl) and refined 2θ, ω, χ values in the range $17 \le \lvert 2\theta \rvert \le 26°$ (λ(Mo K$\bar{\alpha}$) = 0.710 73 Å)	
	(B) Measurement of Intensity Data	
radiation	Mo K$\bar{\alpha}$, graphite monochromator	
reflections measured	$+h$, $+k$, $\pm l$ ($3 \le 2\theta \le 50°$)	$+h$, $+k$, $\pm l$ ($3 \le 2\theta \le 50°$)
scan type, speed	θ–2θ, vble, 2.93–7.33°/min	θ–2θ, vble, 1.95–4.51°/min
scan range	symmetrical, $[1.8 + \Delta(\alpha_2 - \alpha_1)]°$	symmetrical, $[1.9 + \Delta(\alpha_2 - \alpha_1)]°$
no. of reflections measured	1562; 1489 in unique set	2405; 2191 in unique set
standard reflections; period	008, 141, 600; 74	00$\bar{8}$, 180, 400; 74
absorption correction	empirical	empirical
transmission factor range	0.903–1.00	0.936–1.00
data reduction: as before[b]	$p = 0.040$	$p = 0.040$
R_{av}	0.022 (0kl reflections)	0.013 (0kl reflections)
no. of data used in refinement	799 [I > 1.96σ(I)]	1566 [I > 1.96σ(I)]
no. of refined parameters	142	268
weighting of reflections	as before[c]	
solution	SHELXS-86, difference-Fourier	SHELXS-86, difference-Fourier
refinement[d]	full-matrix least-squares	full-matrix least-squares
anisotropic disp params	all non-hydrogen atoms	all non-hydrogen atoms
isotropic disp params	H atoms	H atoms (N, O); fixed H atoms (C)
secondary ext param	$1.2(3) \times 10^{-6}$	$8.4(9) \times 10^{-7}$
R	0.047	0.040
R_w	0.047	0.044
SDU	1.40	1.38
R (*all* reflections)	0.136	0.074
final difference map:	random pks, −0.14 – +0.16 e$^-$/Å^3	−0.18 – +0.17 e$^-$/Å^3

[a] Measured by neutral buoyancy in n-hexane–CH_2Br_2; $CH_2Cl_2 - CH_2Br_2$. [b] Foxman, B. M.; Goldberg, P. L.; Mazurek, H. *Inorg. Chem.* **1981**, *20*, 4368; all computations in the present work were carried out using the ENRAF-NONIUS Structure Determination Package and SHELXS-86: Sheldrick, G. M. *Acta Crystallogr., Sect. A: Found. Crystallogr.* **1990**, *46*, 467. [c] Corfield, P. W. R.; Doedens, R. J.; Ibers, J. A. *Inorg. Chem.* **1967**, *6*, 197. [d] $R_{av} = \sum|I - I_{av}|/\sum I$; $R = \sum||F_o| - |F_c||/\sum|F_o|$; $R_w = \{\sum w[|F_o| - |F_c|]^2/\sum w|F_o|^2\}^{1/2}$. SDU $= \{\sum w[|F_o| - |F_c|]^2/(m - n)\}^{1/2}$, where m is the number of observations and n is the number of parameters.

Table 2. Atomic Coordinates for $(C_5H_7N_2)^+(C_3HO_2)^-$ (4)[a]

atom	x	y	z	B (Å^2)
O1	0.0457(2)	0.2423(3)	0.4269(2)	5.28(5)
O2	0.0191(2)	0.1579(3)	0.2248(2)	5.77(5)
N1	−0.1977(2)	0.1607(4)	0.3834(2)	3.94(5)
N2	−0.2414(2)	0.1606(4)	0.1636(2)	4.96(6)
C1	0.0774(2)	0.2340(5)	0.3291(3)	4.25(7)
C2	0.1938(2)	0.3292(5)	0.3400(2)	4.44(7)
C3	0.2850(3)	0.4106(5)	0.3484(3)	5.63(9)
C4	−0.2812(2)	0.1569(4)	0.2627(2)	3.67(6)
C5	−0.4071(2)	0.1495(5)	0.2480(3)	4.55(7)
C6	−0.4404(2)	0.1442(5)	0.3531(3)	5.44(8)
C7	−0.3522(3)	0.1476(5)	0.4770(3)	5.86(8)
C8	−0.2326(3)	0.1551(5)	0.4889(3)	5.01(8)
H(N1)	−0.107(2)	0.171(4)	0.397(2)	6.1(7)
HA(N2)	−0.152(2)	0.160(4)	0.181(2)	5.4(6)
HB(N2)	−0.299(2)	0.171(4)	0.085(2)	5.3(6)
H3	0.353(2)	0.480(5)	0.352(2)	8.0(9)
H5	−0.464(2)	0.145(4)	0.162(2)	5.0(6)
H6	−0.530(2)	0.147(4)	0.339(2)	6.5(7)
H7	−0.376(2)	0.153(4)	0.549(2)	7.2(8)
H8	−0.159(2)	0.164(4)	0.573(2)	5.6(7)

[a] Atoms refined using anisotropic displacement parameters are given in the form of the isotropic equivalent displacement parameter defined as $1.33[a^2B_{11} + b^2B_{22} + c^2B_{33} + ab\cos\gamma B_{12} + ac\cos\beta B_{13} + bc\cos\alpha B_{23}]$.

The molecules are linked by N2–HB(N2)···O1 [$x - {}^1/_2$, ${}^1/_2 - y$, $z - {}^1/_2$] hydrogen bonds to form infinite chains (Figure 2). The N–H···O angle is 163(2)° with a N···O distance of 2.979(2) Å. Further hydrogen bonding links the propynoate moieties in a head-to-tail fashion by C3–H3···O2 [${}^1/_2 - x$, ${}^1/_2 + y$, ${}^1/_2 - z$] interactions in a herringbone pattern along the b axis (Figure 3). The C–H···O angle is 157(2)° with a C···O distance of 3.161(4) Å.

Crystal and Molecular Structure of 5. The molecular structure of **5** (Figure 4) verifies that the acrylate moiety is bonded to the pyridinium nitrogen atom rather than the amine nitrogen atom. The pyridine portions of the two symmetry-independent molecules (hereafter designated as molecules A and B) are nearly related by a translation of ≈(0.5,0,0). The near translational symmetry of the molecules is broken by a difference in torsional angles about the Cn6–Nn1 bond for the acrylate/pyridinium junction. The torsional angles of molecules A and B are +138.0(3)° and −133.7(3)°, respectively. The expected nonplanarity of the pyridinium molecules[13] arises from the *anti*-aromatic character of the pyridine ring in conjunction with a more sterically favorable orientation of the acrylate substituent. Bond lengths and angles for the two symmetry independent molecules do not differ

---

(13) Razenberg, H.; Kanters, J. A.; Schoone, J. C.; Duisenberg, A. J. M. *Acta Crystallogr., Sect. C: Cryst. Struct. Commun.* **1983**, *39*, 114.

Table 3. Atomic Coordinates for $C_8H_8N_2O_2 \cdot H_2O$ (5)

atom	x	y	z	B (Å²)
OW1	0.3648(2)	−0.4673(2)	0.1828(3)	4.26(6)
OW2	0.8653(2)	−0.4666(2)	0.1978(3)	4.26(6)
O11	0.4342(1)	−0.0887(1)	0.0654(3)	3.05(4)
O12	0.4232(1)	−0.1089(1)	0.3695(3)	3.33(5)
O21	0.9282(1)	−0.1106(1)	0.0632(3)	3.67(5)
O22	0.9354(1)	−0.0903(1)	0.3765(3)	3.07(5)
N11	0.3533(1)	0.1713(1)	0.1287(3)	2.14(5)
N12	0.4873(2)	0.2334(2)	0.0939(3)	2.95(5)
N21	0.8515(1)	0.1680(1)	0.2349(3)	2.10(5)
N22	0.9839(2)	0.2320(1)	0.3908(3)	2.93(6)
C11	0.4051(2)	0.2420(2)	0.1179(3)	2.19(6)
C12	0.3681(2)	0.3240(2)	0.1377(4)	2.64(6)
C13	0.2843(2)	0.3324(2)	0.1612(4)	2.85(7)
C14	0.2320(2)	0.2590(2)	0.1684(4)	2.92(7)
C15	0.2672(2)	0.1808(2)	0.1524(4)	2.72(6)
C16	0.3881(2)	0.0858(2)	0.1167(4)	2.29(6)
C17	0.3734(2)	0.0222(2)	0.2273(4)	2.53(6)
C18	0.4135(2)	−0.0656(2)	0.2191(4)	2.32(6)
C21	0.9022(2)	0.2394(2)	0.2895(4)	2.21(6)
C22	0.8649(2)	0.3208(2)	0.2298(4)	2.49(6)
C23	0.7819(2)	0.3270(2)	0.1234(4)	2.96(7)
C24	0.7307(2)	0.2527(2)	0.0736(4)	2.88(7)
C25	0.7664(2)	0.1753(2)	0.1309(4)	2.55(6)
C26	0.8874(2)	0.0834(2)	0.2829(4)	2.36(6)
C27	0.8780(2)	0.0205(2)	0.1574(4)	2.75(7)
C28	0.9167(2)	−0.0671(2)	0.2045(4)	2.46(6)
HA(OW1)	0.396(3)	−0.453(3)	0.297(6)	10(1)
HB(OW1)	0.390(2)	−0.437(2)	0.096(5)	7.0(9)
HA(OW2)	0.899(2)	−0.440(2)	0.297(4)	4.3(7)
HB(OW2)	0.897(3)	−0.450(2)	0.096(6)	9(1)
HA(N12)	0.515(2)	0.181(2)	0.065(4)	4.2(7)
HB(N12)	0.525(2)	0.284(2)	0.108(4)	4.2(7)
HA(N22)	1.013(2)	0.286(2)	0.413(5)	6.2(9)
HB(N22)	1.011(2)	0.181(2)	0.451(4)	4.2(7)

Table 4

(A) Bond Lengths (Å) for $(C_5H_7N_2)^+(C_3HO_2)^-$ (4)

atom 1	atom 2	dist	atom 1	atom 2	dist
O1	C1	1.256(4)	C3	H3	0.91(3)
O2	C1	1.237(3)	C4	C5	1.401(4)
N1	C4	1.349(3)	C5	C6	1.344(5)
N1	C8	1.358(4)	C5	H5	0.95(2)
N1	H(N1)	1.00(3)	C6	C7	1.395(4)
N2	C4	1.325(4)	C6	H6	0.99(3)
N2	HA(N2)	0.97(2)	C7	C8	1.336(4)
N2	HB(N2)	0.90(2)	C7	H7	0.93(3)
C1	C2	1.463(4)	C8	H8	1.02(2)
C2	C3	1.169(4)			

(B) Bond Lengths (Å) for $C_8H_8N_2O_2 \cdot H_2O$ (5)

atom 1	atom 2	dist	atom 1	atom 2	dist
OW1	HA(OW1)	0.89(4)	N21	C26	1.437(3)
OW1	HB(OW1)	0.92(4)	N22	C21	1.324(3)
OW2	HA(OW2)	0.89(3)	N22	HA(N22)	0.95(3)
OW2	HB(OW2)	0.99(4)	N22	HB(N22)	0.95(3)
O11	C18	1.256(4)	C11	C12	1.414(4)
O12	C18	1.248(3)	C12	C13	1.347(4)
O21	C28	1.256(4)	C13	C14	1.402(4)
O22	C28	1.254(3)	C14	C15	1.344(4)
N11	C11	1.369(3)	C16	C17	1.311(4)
N11	C15	1.383(4)	C17	C18	1.503(4)
N11	C16	1.440(4)	C21	C22	1.416(4)
N12	C11	1.323(4)	C22	C23	1.352(4)
N12	HA(N12)	0.96(3)	C23	C24	1.402(4)
N12	HB(N12)	0.96(3)	C24	C25	1.348(4)
N21	C21	1.365(3)	C26	C27	1.311(4)
N21	C25	1.374(3)	C27	C28	1.494(4)

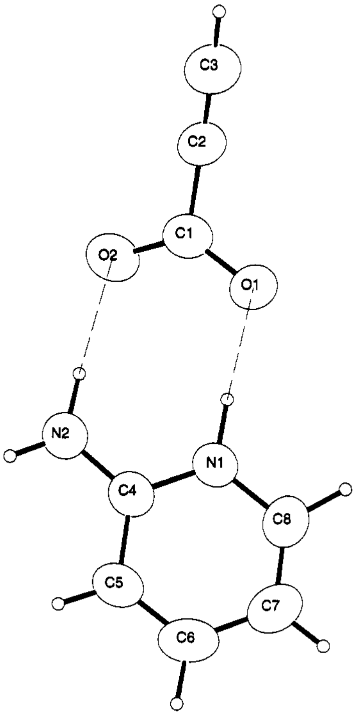

Figure 1. Molecular structure and numbering scheme for 2-aminopyridinium propynoate (4).

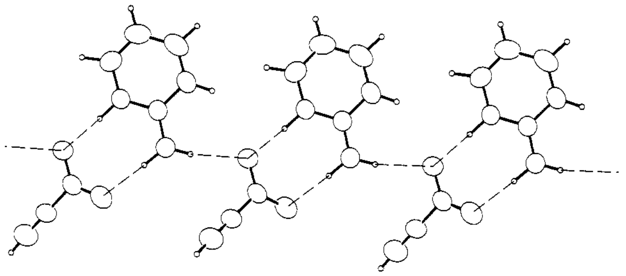

Figure 2. N–H···O′ hydrogen-bond pattern for 2-aminopyridinium propynoate (4).

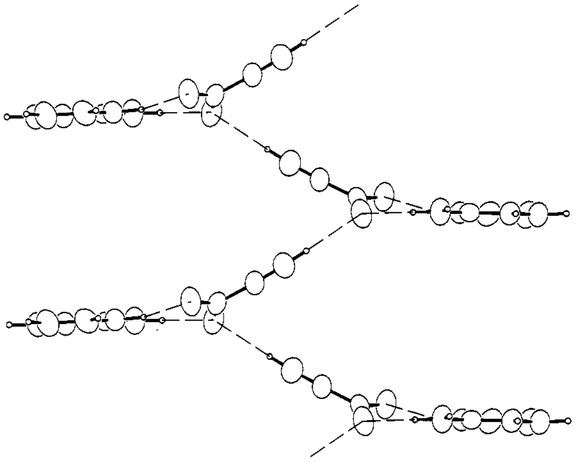

Figure 3. C–H···O hydrogen-bond pattern for 2-aminopyridinium propynoate (4).

significantly (Table 4). Therefore, the following discussion will consider only molecule A, unless otherwise specified. The sum of the angles around the amine nitrogen atom, N12, is 360(2)°, suggesting sp^2 character for that atom. The amino nitrogen-to-ring bond length N12–C11, 1.323(4) Å, is significantly shorter than the N–C distances within the ring (1.369(3) and 1.383(4) Å). The C–C distances within the ring also show a deviation from normal aromatic pyridine structures.[12] The distances C12–C13 (1.347(4) Å) and C14–C15 (1.344(4) Å) are significantly shorter than C11–C12 (1.414(4) Å) and C13–C14 (1.402(4) Å) bond lengths. This evidence suggests an important contribution from resonance form **8** to the structure of **5** rather than resonance form **9**.

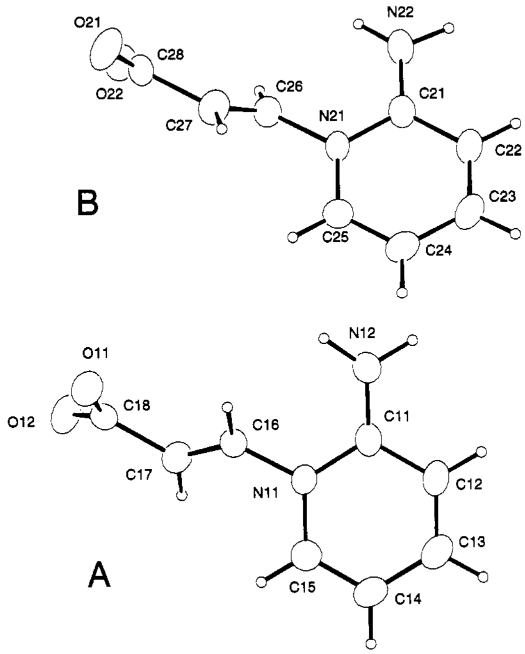

Figure 4. The two symmetry-independent molecules of (*E*)-2-aminopyridinium-1-acrylate (**5**).

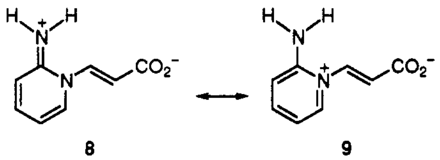

8 **9**

The crystal structure of **5** comprises an intricate arrangement of hydrogen bonds and π–π orbital interactions. The molecules are linked to the water molecules (OW1) by infinite chains of O11···HA(OW1)–OW1 [$x, -^1/_2 - y, z - ^1/_2$] and O12···HB(OW1)–OW1 [$x, -^1/_2 - y, ^1/_2 + z$] hydrogen bonds (Figure 5). The O···H–O angles are 164(4)° and 166(3)°, respectively, with O···O distances of 2.852(3) and 2.836(3) Å. Another mode of hydrogen bonding links pairs of molecules in centrosymmetric, 16-membered ring dimers through pairs of O11···HA(N12)–N12 [$1 - x, -y, -z$] interactions. The O···H–N angle is 164(2)° with an O···N distance of 2.892(3) Å. Additionally, each homodimer is further linked to another dimer by O12···HB(N12)–N12 [$1 - x, y - ^1/_2, ^1/_2 - z$] hydrogen bonds (Figure 6). The O···H–N angle is 169(3)° with an O···N distance of 2.796(3) Å. Inspection of Figure 6 reveals an apparent parallel alignment of pyridinium planes; the pyridinium rings [$x, ^1/_2 - y, z - ^1/_2$] are positioned ≈3.6 Å from one another.

Solid-State Reactivity of 4. Compound **4** was exposed to γ-rays using a Gammacell 220 (Atomic Energy of Canada, Ltd.) equipped with a ^{60}Co source. After 23.4 Mrad of γ-irradiation, the ^{1}H NMR spectrum of the irradiated material was identical to that of the starting material **4**. This lack of reactivity contrasts greatly with the sensitivity of *metal* propynoates to ionizing radiation and will be discussed further below.

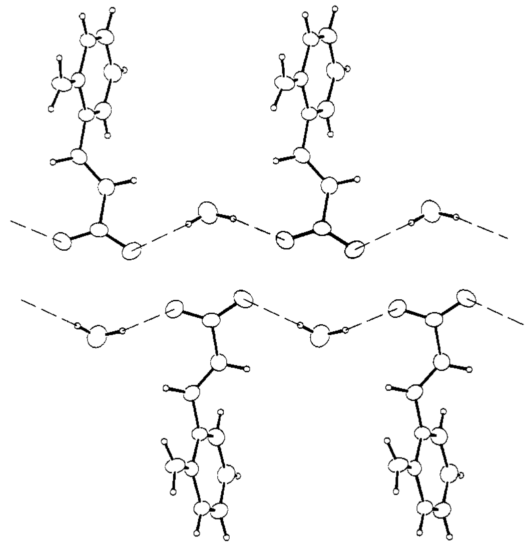

Figure 5. View of **5** showing the *anti–anti* hydrogen bonds to water.

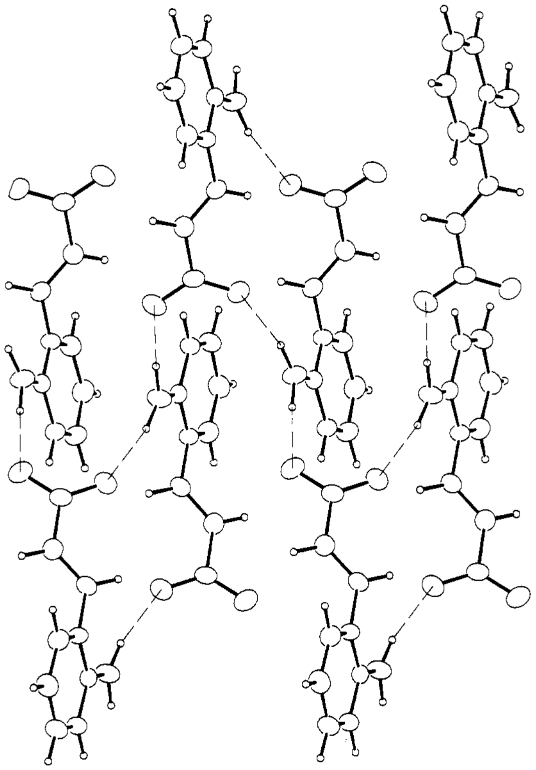

Figure 6. View of N–H···O hydrogen bond scheme and pyridine stacks for **5**.

Table 5. Thermal Behavior of 4

temp (°C)	time (h)	yield (%)	5:6 (*E*:*Z*)
60	2.0	15	2.5
	6.0	15	2.5
	22.5	22	2.5
80	2.0	50	1.4
	6.0	80	1.4
	23.0	100	1.4
100	2.0	100	0.9
	6.0	100	0.9
	19.0	100	0.9

As a next step, we decided to investigate the thermal reactivity of **4**. Heating solid **4** affords the *E* and *Z* products (**5** and **6**, respectively) in ≈100% yield at 125 °C. To the best of our knowledge, this is only the second such addition observed to occur in the solid state. Table 5 shows the behavior of **4** at 60, 80, and 100 °C, with reaction yields and product ratios obtained from integration of ^{1}H NMR spectra. Note both the dependence of the *E*:*Z* product ratio on temperature and the increase in rate of reaction and yield with increasing temperature. At 60 °C the ratio is 2.5:1, at 80 °C 1.4:1, and at 100 °C the ratio is 0.9:1. It is worth noting that the product ratios do not change with heating times for each specific reaction temperature. In the analogous solution reaction, Wilson and Bottomley[14] discovered that the reaction of methyl propynoate with 2-aminopyridine resulted in **5**, **6**, and **10**(8.2:15.0:12.6) in

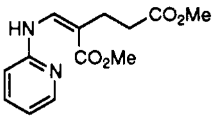

10

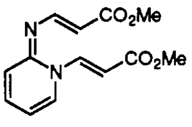

11

a 36% combined yield. A fourth product (**11**) was observed, but no yield was reported. The solid-state reaction with **4** is *considerably* more selective and results in the formation of only the *E* (**5**) and *Z* (**6**) isomers in quantitative yields. This discussion of course assumes that the *Z* isomer readily cyclizes to pyridopyrimidone **6**. The molecular structure of **6** was easily confirmed by comparison of the ^{1}H NMR chemical shifts and coupling constants to that of analogous compounds.[15] On the other hand, the structure of the second product could not be substantiated as **5** from analysis of NMR data, since a similar spectral pattern would be expected for **12**.[15] We

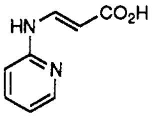

12

were confident, however, that the product was an *E* acrylate; this conclusion was based upon the large (13.7 Hz) coupling constant observed for the δ 7.54 and 6.57 resonances. As described above, we demonstrated that **5** was the correct formulation by an X-ray structure determination.

Even though the dependence of product distribution on temperature suggests that the process occurs in the solid state, we initially could not rule out the possibility that the reaction occurred in the melt. Analysis of differential scanning calorimetry (DSC) data for **4** shows unambiguously that the reaction took place in the solid state. An endotherm at 81.1 °C corresponds to the solid-state reaction, and a peak at 122–123 °C is attributed to melting. The thermogravimetric analysis (TGA) of **4** indicates no weight loss prior to melting.

In the crystal structure of **4**, short C–H···O intermolecular hydrogen bonds link acetylenic moieties in an infinite chain. This arrangement creates an infinite chain of short (3.653(5) Å) acetylenic C2···C3′ interactions $[{}^1/_2 - x, y - {}^1/_2, {}^1/_2 - z]$ (Figure 3). With such short contacts between propynoate moieties, one would expect the material to undergo a solid-state polymerization reaction upon irradiation with X- or γ-rays. Nonetheless, the material has been shown to be stable in the presence of ionizing radiation. This result indicates that an increase in the ionic character of the propynoate moiety (*cf.* neutral organic acetylenes[5]) is *not* an important influence upon the onset of solid-state reactivity. For the analogous metal propynoates, this suggests that the metal cation plays a key role, perhaps as primary absorber of the ionizing radiation, in (at least) the initiation of activation of the propynoate moiety toward polymerization.

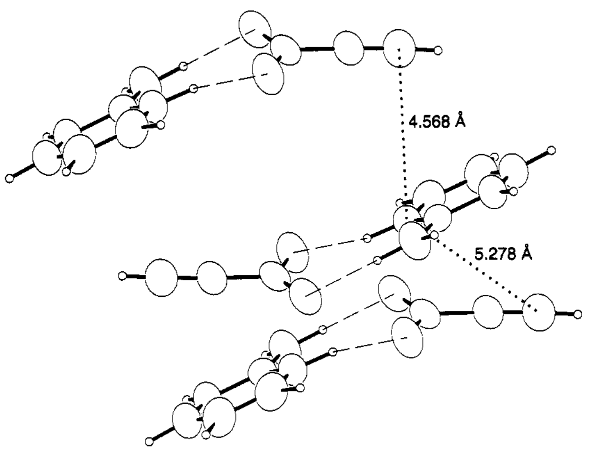

Figure 7. Molecular arrangement of 2-aminopyridinium propynoate (**4**) showing the shortest C3···N1 contacts.

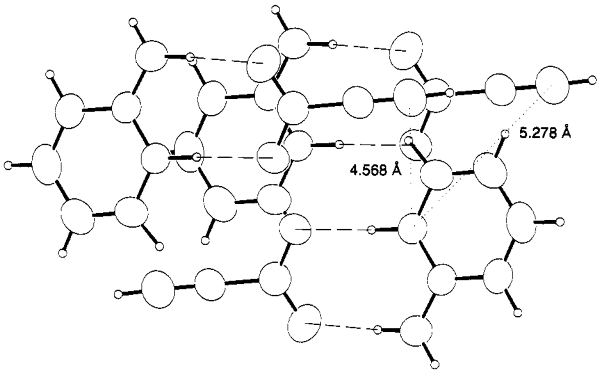

Figure 8. Molecular arrangement of 2-aminopyridinium propynoate (**4**) showing the shortest C3···N1 contacts. A view ⊥ to Figure 7.

The thermally induced solid-state reaction of **4** presents a challenging opportunity to propose a possible reaction pathway from crystallographic data. To understand the solid-state reaction (or reaction pathway) of **4**, a detailed study of intermolecular contacts was undertaken. In general, the reaction is viewed as a three-step process: (i) deprotonation of the pyridinium nitrogen atom, (ii) addition of the lone pair of the pyridine nitrogen atom to the triple bond, and (iii) proton transfer to form either the *E* (**5**) or *Z* isomer (*Z* isomer cyclizes to form **6**). In the first step, the proton attached to the pyridinium nitrogen atom is abstracted by the carboxylate oxygen atom of the complex, where the H···O1 distance is 1.75(3) Å (N1···O1, 2.733(3) Å). The nearest intermolecular contact, 3.634(4) Å, N2···C3 $[x - {}^1/_2, {}^1/_2 - y, z - {}^1/_2]$, is between the imine nitrogen atom and the β-carbon atom of the propynoate (see Figure 2). However, reaction only occurs between the pyridine nitrogen and the β-carbon atom of the propynoate. The three shortest N1···C3 distances and the associated symmetry operations are N1···C3 $[\bar{x}, 1 - y, 1 - z]$, 4.568 Å; N1–C3 $[x - {}^1/_2, {}^1/_2 - y, {}^1/_2 + z]$, 5.235(4) Å; and N1–C3 $[\bar{x}, \bar{y}, 1 - z]$, 5.278 Å. The C2–C3···N1 angles for these contacts are 88.8(2), 102.3(2) and 48.4(2)°, respectively. The first and third of these are shown in Figures 7 and 8. The criteria established for UV, X-ray, and γ-ray initiated solid-state reactions (distances <≈4.2 Å) would suggest this arrangement to be stable. It is unlikely that such criteria apply for a thermal reaction of this type,

---

[14] Wilson, J. G.; Bottomley, W. *J. Heterocycl. Chem.* **1967**, 360.

[15] (a) Pollak, A.; Stanovnik, B.; Tisler, M. *J. Org. Chem.* **1971**, *36*, 2457. (b) Kinoshita, T.; Ueshima, Y.; Saitoh, K.; Yoshida, Y.; Furukawa, S. *Chem. Pharm. Bull.* **1987**, *35*, 90.

given that molecular motion in the crystal is of greater importance.

Without additional structural information to guide us in our thinking, it seems reasonable to consider that the shortest N1···C3 contact is the most important. The C2–C3···N1 angle of 88.8° is midway between the value (60°) proposed by Baldwin for ring closures of alkynes;[16] however, this value was revised (120°) by Eisenstein, Procter, and Dunitz for nucleophilic addition to a triple bond.[17] Obviously, a new calculation would be highly desirable. In addition to a new theoretical result, the ultimate answer to such questions must await a full study of the solid-state reactivity of related cocrystals and/or cocrystalline salts of alkynoic acids, now underway in our laboratories.

Appendix

Here we present a detailed description of the hydrogen bond patterns for **4** and **5** in terms of the graph set methodology developed by Etter, Bernstein, and coworkers.[18] This scheme allows the straightforward classification of hydrogen-bonding patterns and has been used in the characterization of a host of systems.[19] A logical progression of the graph theory has been applied to more complicated systems, such as structures that contain more than one molecule per asymmetric unit.[20] This extension analyzed hydrogen bonds at different levels (i.e., unitary, binary, ternary, etc.). Hydrogen-bond patterns at the unitary level are classified by one specific type of interaction; binary hydrogen-bond patterns are characterized by two interactions. The symbol to be used is $\mathbf{G}_{\mathbf{d}}^{\mathbf{a}}(\mathbf{r})$, where the pattern designator **G** = **D**iscrete, **C**hain, **R**ing or **S**elf; the characters **a** and **d** specify the number of donor and acceptor atoms involved in the hydrogen-bond pattern, and **r** is the total number of atoms involved in the hydrogen bond pattern.

Analysis of the hydrogen bond patterns for **4** shows the graph sets to be **DDC(5)** at the unitary level. The three discrete hydrogen bonds are N2–HA(N2)···O2, N2–HB(N2)···O1 and N1–H(N1)···O1 (Figures 1 and 2). Further hydrogen bonding links the propynoate moieties in a head-to-tail fashion by C3–H3···O2 hydrogen bonds in a herringbone pattern, a **C(5)** chain along *b* (Figure 3). The binary level is characterized by $\mathbf{C}_2^1(6)\mathrm{C}_2^2(6)\mathbf{R}_2^2(8)$ graph sets. Two unique chains, $\mathbf{C}_2^1(6)$ and $\mathbf{C}_2^2(6)$, are formed by N2–HB(N2)···O1, N2–HA(N2)···O2 and N2–HB(N2)···O1, N1-H(N1)···O1 pathways (Figure 2). Additionally, the 2-aminopyridinium and propynoate ions form a *nonplanar*, eight-membered ionic complex ($\mathbf{R}_2^2(8)$, Figure 1).

As discussed above, the crystal structure of **5** contains two symmetry-independent monohydrated moieties. The hydrogen bond patterns for each complex do not differ significantly; a detailed description of only one of the systems follows. Analysis of the patterns generated from the hydrogen bond sets described for **5** (*vide supra*) determines the graph sets to be $\mathbf{DDC(8)R}_2^2\mathbf{(16)}$ at the unitary level. The two discrete hydrogen bond units involve the water H atoms (OW1–HA(OW1)···O11 and OW1–HB(OW1)···O12). Hydrogen bonding links the (*E*)-2-aminopyridinium-1-acrylate groups by N12–HB(N12)···O12 interactions, a **C(8)** chain, along the *b* axis. These chains are further linked by N12–HA(N12)···O11 hydrogen bonds to form a $\mathbf{R}_2^2(16)$ ring system. At the binary level, the graph sets for **5** are $\mathbf{C}_2^2(6)\mathbf{C}_2^2(6)$. Infinite chains consisting of OW1–HA(OW1)···O11 and OW1–HB(OW1)···O12 interactions link the acrylate groups along the *c* axis, and further linking occurs (through N12–HB(N12)···O12, and N12-HA(N12)···O11 interactions) along *b*. The formation of these rings and chains create an undulated sheet of acrylate moieties and water molecules in the *bc* plane. These sheets are interleaved by similar layers (with identical graph sets) consisting of the other symmetry independent (*E*)-2-aminopyridinium-1-acrylate and water molecules.

Acknowledgment. We thank the National Science Foundation (DMR-9221487) for the support of this research, Professor B. B. Snider for helpful discussions, and Mr. Paul Gendron of Polaroid Corp. for carrying out the DSC experiments. K.A.W. is most grateful to Professor Etter for stimulating his interest in solid-state chemistry during his career as an undergraduate at the University of Minnesota.

Supplementary Material Available: Tables of anisotropic displacement parameters, all bond lengths and angles, and calculated H atom positions for structure 4 and 5 (6 pages); list of observed and calculated structure factors for structures 4 and 5 (9 pages). Ordering information is given on any current masthead page.

---

(16) Baldwin, J. E. *J. Chem. Soc., Chem. Commun.* **1976**, 734.

(17) Eisenstein, O.; Procter, G.; Dunitz, J. D. *Helv. Chim. Acta* **1978**, *61*, 2538.

(18) (a) Etter, M. C. *Acc. Chem. Res.* **1990**, *23*, 120 and references therein. (b) Reutzel, E.; Etter, M. C. *J. Am. Chem. Soc.* **1991**, *113*, 2586. (c) Etter, M. C.; MacDonald, J. C.; Bernstein, J. *Acta Crystallogr., Sect. B: Struct. Sci.* **1990**, *46*, 256.

(19) (a) Panunto, T. W.; Urbanczyk-Lipkowska, Z.; Johnson, R.; Etter, M. C. *J. Am. Chem. Soc.* **1987**, *109*, 7786. (b) Zerkowski, J. A.; Seto, C. T.; Wierda, D. A.; Whitesides, G. M. *J. Am. Chem. Soc.* **1990**, *112*, 6409. (c) Etter, M. C.; Panunto, T. W. *J. Am. Chem. Soc.* **1988**, *110*, 5896. (e) LeChat, J. R.; de Almeida Santos, R. H. Bueno, W. A. *Acta Crystallogr., Sect. B: Struct. Sci.* 1981, *37*, 1468.

(20) Bernstein, J.; Davis, R. E.; Shimoni, L.; Chang, N. L., manuscript in preparation.